Effect of anode MPL on water and methanol transport in DMFC: Experimental and modeling analyses

M. Zago[*], *A. Casalegno*, *F. Bresciani*, *R. Marchesi*

Politecnico di Milano, Department of Energy, via Lambruschini 4, 20156 Milano, Italy

Received 30 January 2014
Received in revised form
10 March 2014
Accepted 19 March 2014
Available online 18 April 2014

Introduction

The Direct Methanol Fuel Cell (DMFC) is a promising energy source for portable and automotive applications, mainly due to the direct use of a liquid fuel, quick recharging and low operating temperature [1–3]. However the widely use of the DMFC technology is still hindered by some technological issues, among which one of the most important is related to the regulation of mass transport of different species through the anode Diffusion Layer (DL) and the membrane. Mass transport not only affects the performance, but also influences the operating stability of the system [4,5].

DMFCs are fed at the anode with a liquid mixture composed by water and methanol; both species flow through the membrane from anode to cathode. Water crossover through the membrane may cause two problems: cathode flooding and excessive anodic water consumption [6–9]. The former decreases oxygen diffusivity at cathode, lowering the cell voltage, the latter enhances methanol crossover through the membrane, increasing fuel waste.

During the last years, both water and methanol crossover in DMFCs have been extensively studied [10–22]. It has been found that the design of anode DL plays an important role in controlling water and methanol crossover. The former is due to three transport mechanisms: electro-osmotic drag by proton transport, diffusion by water concentration gradient and convection by hydraulic pressure gradient [23,24]. The latter, instead, mainly depends on diffusion across the membrane and it can be minimized reducing the methanol concentration

* *Corresponding author*.
E-mail addresses: matteo1.zago@polimi.it, zago.matte@gmail.com (M. Zago).

in the anode electrode. For these reasons anode Gas Diffusion Layer (GDL) can be coated with an additional highly hydrophobic Micro Porous Layer (MPL), that acts as a liquid barrier to the Catalyst Layer (CL), reducing both water and methanol crossover through the membrane.

On the other hand a too low methanol concentration in the anode CL can result in a large mass transport loss, worsening the cell voltage. Hence, maintaining an adequate methanol concentration in the anode CL is critical to minimize both the rate of methanol crossover and the mass transport loss.

Therefore a detailed and consolidated comprehension of the phenomena regulating methanol and water transport through anode DL is fundamental, permitting to further optimize components and operation strategies. For this reason also modeling analysis deals with DMFC [25–35]. However the most of developed models are validated on few experimental results, strongly limiting the model effectiveness in fuel cell design and optimization. Moreover the most of the DMFC models analyze the effect of cathode DL properties on DMFC operation [28–33], while the anode is less investigated [14,34,35]. C.Y. Wang et al. [14,35] presented a 1D two-phase transport model to study the effects of anode MPL transport properties on water crossover; however the models are not integrated along channel length. X.Y. Li et al. [34] developed a two-dimensional two-phase model to analyze the effect of anode MPL on both methanol and water crossover, but no attempts to fit experimental data have been done.

This work aims to improve and consolidate the understanding of water and methanol transport phenomena through the anode DMFC components and to suggest improvements of anode DL. A previously developed 1D + 1D DMFC isothermal model [36,37] is integrated with a detailed description of methanol and water transport through anode DL and validated over a wide range of operating conditions with respect to three typologies of measures: performance, water transport and methanol crossover.

The work is organized as follows: in Section 2 the experimental results regarding water and methanol transport are reported; in Section 3, the model improvement is described; in Section 4, the main model results are analyzed and discussed and finally some conclusions are given in Section 5.

Experimental analysis

Experimental setup

The experimental analyses of DMFC water transport and methanol crossover are carried out in the same equipment previously developed in Ref. [38]. The MEA was purchased already assembled by BalticFuelCells GmbH with an active area of 22.1 cm^2, consisting of Pt–Ru anode (4 mg cm^{-2}, Pt:Ru = 2), a Nafion® 117 membrane and Pt cathode (4 mg cm^{-2}). Both anode and cathode DL are coated with MPL (Sigracet® SGL10CC): for this reason this MEA is named MEA MM, as in previous publication [38].

Table 1 – Investigated operating conditions (MEA MM: MPL on both anode and cathode).

MEA	T [K]	X_{CH_3OH} [%wt]	m_{air} [g/min]	p^c_{in} [kPa]	p^c_{out} [kPa]
MM	333	3.25	0.62	112	108
MM	333	3.25	1.14	122	115
MM	333	6.5	0.62	112	108
MM	333	6.5	1.14	122	115
MM	353	3.25	0.62	112	108
MM	353	3.25	1.14	122	115
MM	353	6.5	0.62	112	108
MM	353	6.5	1.14	122	115

Water transport analysis

The tested operating conditions are reported in Table 1: in all of them the anode flow rate is set at 1 g min^{-1} and the anode mean pressure at 105 kPa.

In Fig. 1 the water flow at cathode outlet, in function of current density, is reported for different operating conditions. The water flow of MEA MM is nearly constant as the current density changes, a sort of plateau is evident: this implies that water transport through cathode GDL is mainly governed by gas diffusion, as already proposed in Ref. [37]. This behavior is coherent with the following considerations regarding Fig. 1:

- an increase of airflow rate induces a decrease of water concentration in cathode channel, as a consequence the water concentration difference across the GDL and the relative diffusive flow grow; therefore the water flow at cathode outlet, i.e. the plateau value, increases;
- an increase of temperature determines a general increment of both GDL diffusivity and water concentration at cathode electrode, related to saturation concentration; thus the water flow at cathode outlet increases;
- at higher methanol concentration the water flux at cathode outlet does not vary, the water flux is slightly affected by methanol feeding concentration.

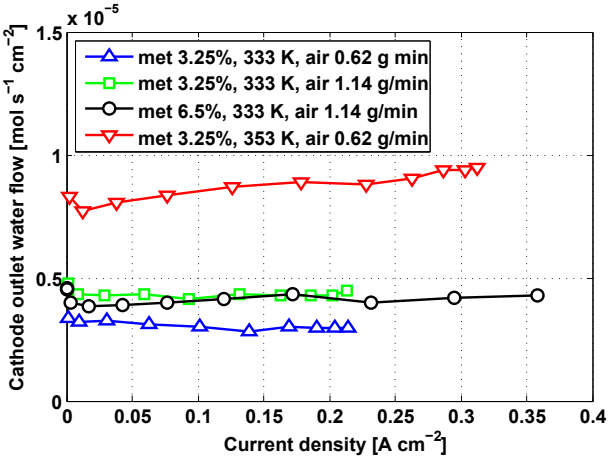

Fig. 1 – Influence of operating conditions on water flux (MEA MM: MPL on both anode and cathode).

Fig. 2 reports a comparison between the water flow at cathode outlet of MEA MM and MEA GM (GDL without MPL at anode and GDL with MPL at cathode, already analyzed in Ref. [37]) in two extremely different operating conditions.

In MEA GM the water transport presents a plateau, due to vapor diffusion, and a linear trend, caused by liquid permeation, as demonstrated in Ref. [37]. Considering MEA MM a reduction of water transport is evident: this feature is coherent with a lower water crossover through the membrane, due to the presence of a liquid water barrier to the anode (i.e., the MPL). Moreover the plateau value decreases: the reduced water crossover lowers cathode water concentration. The absence of an evident linear trend in MEA MM implies that most probably liquid permeation through cathode DL does not occur and therefore there is no effect of bulk pore obstruction [37] on the performance.

Methanol transport analysis

Water management could affect not only performance, but also methanol crossover. Methanol crossover values reported in Fig. 3 are consistent with the water transport results of Fig. 2: an enhanced water flux at cathode outlet causes an increase of the anode average methanol concentration. Coherently with this dilution mechanism, MEA GM exhibits a higher methanol crossover than MEA MM. However the magnitude of dilution effect is not sufficient to cause such a marked reduction of methanol crossover: the presence of anode MPL increases mass transfer resistance entailing a further reduction of average methanol concentration in the electrode.

Modeling analysis

The proposed experimental analysis evidences the importance of anode DL configuration in controlling both water and methanol crossover. In the literature, the mechanisms regulating mass transport phenomena through anode DL are not fully consolidated and a detailed comprehension of such phenomena is required to further optimize components and operation strategies. In order to analyze the mass transport phenomena through anode DL a specific modeling analysis is reported in the followings.

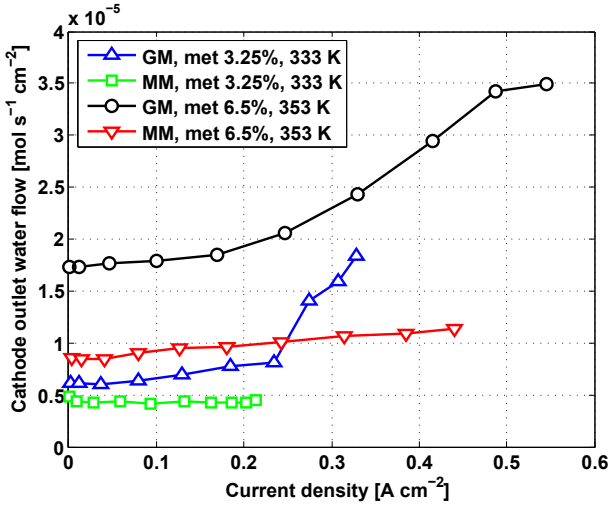

Fig. 2 – Influence of anode MPL on water flux, airflow 1.14 g min^{-1}, (Δ and ○ are taken from Ref. [37]).

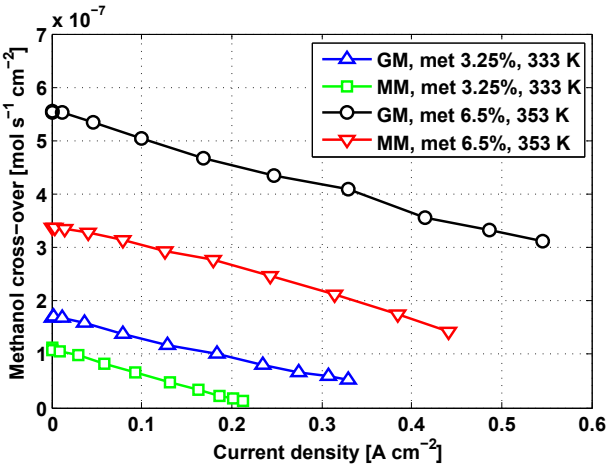

Fig. 3 – Influence of anode MPL on methanol crossover, airflow 1.14 g min^{-1}, (Δ and □ are taken from Ref. [38]).

Model development

A previously developed 1D + 1D DMFC model [36,37] is integrated with a detailed description of methanol and water transport phenomena through anode DL, composed by GDL and MPL.

Anode DL model

In the 1D + 1D DMFC isothermal models presented in Refs. [36,37], due to the high water availability at the anode, the phenomena governing water transport through anode DL was omitted; the water transport through the MEA was assumed in the investigated conditions to be regulated by water transport through the membrane and the cathode DL. Moreover in such model, the methanol flux through the anode DL is governed by gas and liquid diffusion, assuming that liquid saturation is constant across DL thickness (Eq. (18) in Ref. [36]).

In this work the following improvements have been introduced:

- the water is transported through the anode DL by liquid convection: however the water transport through the MEA is still regulated by water transport through the membrane and cathode DL, coherently with the previously proposed interpretations on water transport phenomena [37];
- the contribution of methanol liquid convection through anode DL is considered;
- liquid saturation is no longer constant across the anode DL thickness due to the liquid convective fluxes.

The equations that describe methanol and water transport phenomena through anode DL are the following:

$$-D^{L}_{DL,CH_3OH}\cdot s_{DL}\cdot\frac{\partial C^{DL,L}_{CH_3OH}}{\partial x}-D^{G}_{DL,CH_3OH}\cdot(1-s_{DL})\cdot\frac{\partial C^{DL,G}_{CH_3OH}}{\partial x}=N^{CH_3OH}_{DL}-N^{H_2O}_{DL}\cdot\frac{C^{DL,L}_{CH_3OH}}{C^{DL,L}_{H_2O}} \quad (1)$$

$$\frac{\partial s_{DL}}{\partial x}=\frac{1}{s^3_{DL}\cdot(1.417-4.24\cdot s_{DL}+3.789\cdot s^2_{DL})}\cdot\frac{M_{H_2O}\cdot\nu_{H_2O}}{\sigma_{H_2O}\cdot\cos\theta_c\cdot(\varepsilon_{DL}\cdot K_{DL})^{0.5}}\cdot N^{H_2O}_{DL} \quad (2)$$

where the subscript/superscript DL refers to the considered layer (i.e. GDL or MPL) and the effective diffusion coefficients are corrected accounting for the porosity and the tortuosity of the DL, as reported in Ref. [39].

Eq. (1) is the Fick's law of diffusion for two-phase methanol, in which the second term in the right hand side of the equation is the contribution of methanol liquid convection. The liquid concentration gradient is proportional to the liquid saturation, while the gas phase one is proportional to the void fraction. As proposed in Ref. [36], the methanol concentrations in gas and liquid phases are considered in equilibrium, described by Henry's law:

$$C^{DL,L}_{CH_3OH}=K_{H,CH_3OH}\cdot C^{DL,G}_{CH_3OH}\cdot R\cdot T \quad (3)$$

Eq. (2) is the governing equation of water transport, that is described by the Leverett function [31]. At the interface of two distinct porous layers (e.g. GDL and MPL), the capillary pressure remains uniform across the interface, as widely accepted in the literature [35,40].

$$p_c\big|_{Int^-}=p_c\big|_{Int^+} \quad (4)$$

According to Ref. [31], the capillary pressure can be expressed as:

$$p_c=\sigma_{H_2O}\cdot\cos\theta_c\cdot(\varepsilon/K)^{0.5}\cdot J(s) \quad (5)$$

where $J(s)$ is the Leverett function and for a hydrophobic medium is given by the following relation:

$$J(s)=1.417\cdot s-2.120\cdot s^2+1.263\cdot s^3 \quad (6)$$

As a result, a saturation jump model is implemented at those interfaces.

Membrane model

As already discussed in section 2, the presence of a highly hydrophobic liquid barrier reduces water crossover through the membrane. As a consequence at the anode interface with the membrane it is no longer possible to assume a fully hydrated membrane (Eq. (8) in Ref. [37]).

As reported in Ref. [41], under the condition of phase equilibrium between the water dissolved in the CL ionomer and the liquid water in the CL pores, the water content in the ionomer of the anode catalyst layer can be related to the anode void fraction by:

$$\lambda^{t,a}=s^{t,a}\cdot\lambda^{L}_{eq}+(1-s^{t,a})\cdot\lambda^{G}_{eq} \quad (7)$$

where λ^{L}_{eq} and λ^{G}_{eq} denote the equilibrium water concentration in the ionomer when the ionomer is in phase equilibrium with the liquid water [42,43] and water vapor saturated gas [30], respectively. According to Refs. [44,45], due to the presence of liquid water at both the anode and the cathode, the water transfer resistance at membrane-DL interfaces is neglected.

Therefore the dissolved water concentration in the ionomer of the anode CL is equal to:

$$C^{t,a,L}_{H_2O}=\frac{\rho_{dry}\cdot\lambda^{t,a}}{EW} \quad (8)$$

where ρ_{dry} and EW denote respectively the density of a dry membrane and the equivalent weight of ionomer in the membrane.

The methanol and water diffusivities through the membrane are respectively equal to [41]:

$$D_{m,CH_3OH}=W_1\cdot 4.17\cdot 10^{-4}\cdot\bar{\lambda}\cdot(161\cdot\exp(-\bar{\lambda})+1)\cdot\exp(-2436/T) \quad (9)$$

$$D_{m,H_2O}=W_2\cdot 4.17\cdot 10^{-4}\cdot\bar{\lambda}\cdot(161\cdot\exp(-\bar{\lambda})+1)\cdot\exp(-2436/T) \quad (10)$$

where W_1 and W_2 have been calibrated over experimental data; $\bar{\lambda}$ is the average water content of the membrane, given by:

$$\bar{\lambda}=(\lambda^{t,a}-\lambda^{t,c})/2 \quad (11)$$

As reported in Refs. [30,46], the water content profile in the membrane is almost liner and therefore the dependence of water and methanol diffusivities on $\bar{\lambda}$ is a reasonable assumption. For the evaluation of membrane proton conductivity the correlation reported in Ref. [47] have been adopted.

$$\sigma_m=(0.46\cdot\bar{\lambda}-0.25)\cdot\exp[-1190\cdot(1/T-1/298.15)] \quad (12)$$

DMFC model

The equations characterizing mass transport phenomena through anode DL and membrane have been introduced in the DMFC model previously developed in Ref. [37]. The DL equations, Eqs. (1)–(2), are solved applying the appropriate boundary conditions regarding methanol concentration and saturation at the channel-GDL interface, $s_{ch\text{-}GDL}$. The complex two-phase hydrodynamics in the channel makes the liquid saturation at this interface difficult to be determined theoretically. In the literature, the most of the works [14,35] suppose its value: in Ref. [35] it is equal to 0.8, while in Ref. [14] it is equal 0.65, despite the lower hydrophobicity of the considered diffusion media. According to Refs. [48,49], also in this work an empirical approach is adopted. The saturation is assumed to

Table 2 – Fitted and assumed modeling parameters.			
$D_{m,CH3OH}$	$1.4 \times 4.17 \times 10^{-4} \times 22 \times (161\exp(-22)+1) \times \exp(-2436/T)$	$cm^2\ s^{-1}$	Calibrated
$D_{m,H2O}$ (MEA MM)	$4.17 \times 10^{-4} \times 22 \times (161\exp(-22)+1) \times \exp(-2436/T)$	$cm^2\ s^{-1}$	Calibrated
$D_{m,H2O}$ (MEA GM)	$0.55 \times 4.17 \times 10^{-4} \times 22 \times (161\exp(-22)+1) \times \exp(-2436/T)$	$cm^2\ s^{-1}$	Calibrated
γ^a	0.35	–	Calibrated
α^a	0.58	–	Calibrated
i^a_*	$1.2 \times 10^{-4} \times \exp(126000/R \times (1/353-1/T))$	$A\ cm^{-2}$	Calibrated
α^c	0.54	–	Calibrated
i^c_*	$2.17 \times \exp(11135/R \times (1/353-1/T))$	$A\ cm^{-2}$	Calibrated
n_d	$2.9 \times \exp(1029 \times (1/333-1/T))$	–	Calibrated
n_{dx}	$0.87 \times \exp(410 \times (1/333-1/T))$	–	Calibrated
S_1	0.85	–	Calibrated
S_2	0.15	–	Calibrated
K_m	2×10^{-18}	m^2	Assumed
l^a_{GDL}	0.02	cm	Assumed
K_{GDL}	1×10^{-12}	m^2	Assumed
θ_{GDL}	110	°	Assumed
ε_{GDL}	0.6	–	Assumed
l^a_{MPL}	0.003	cm	Assumed
K_{MPL}	2×10^{-13}	m^2	Assumed
θ_{MPL}	122	°	Assumed
ε_{MPL}	0.3	–	Assumed
K_{MPL}	7×10^{-14}	m^2	Assumed
θ_{MPL}	99	°	Assumed
ε_{MPL}	0.3	–	Assumed

be dependent on the saturation in the channel; the following correlation is proposed:

$$s_{ch-GDL} = S_1 \cdot s_{ch} + S_2 \tag{13}$$

where s_{ch} is the saturation in the channel and the parameters S_1 and S_2 are calibrated over experimental data.

Model validation

The considered experimental data set for model validation is composed of 88 measurement points, coming from 8 polarization curves of MEA MM, Table 1. The model is calibrated with respect to three different typologies of measure at the same time: performance, water transport and methanol crossover.

Table 2 reports the assumed and fitted parameters. Due to the more detailed description of mass transport phenomena through anode DL and the membrane, that affect the whole DMFC operation, the kinetic and mass transport parameters are different from those reported in Ref. [37]. The resulting values are coherent with those reported in the literature, Table 2. In particular the electro-osmotic drag coefficient can increase considerably when methanol is present [50]: the resulting value of 2.9 [51], lower than that reported in Ref. [37] for MEA GM, is coherent with the reduced methanol concentration in the electrode of MEA MM [50].

A comparison between simulated and experimental results of performance, water transport and methanol crossover in two extremely different operating conditions is reported in Fig. 4(a–c), respectively.

Generally model simulations reproduce experiments with good accuracy. Model simulations of Fig. 4(b) suggest that liquid permeation in MEA MM does not occur and water transport through cathode GDL is mainly governed by gas diffusion mechanism. Moreover gas diffusion slightly increases with the current density: this implies an increase of water concentration in the electrode, that is not close to the saturation value at low current density.

Also methanol crossover simulations are in full agreement with experimental data. The developed model confirms, as widely accepted in the literature [10,52], that the magnitude of methanol liquid diffusion is more relevant than the electro-osmotic one in determining methanol crossover.

Moreover Fig. 4 reports model predictions without the presence of anode MPL (MEA GM); just eliminating the presence of anode MPL the model is once again able to reproduce the experimental data. In these simulations only the value of methanol diffusivity through the membrane is re-calibrated, while the water drag coefficient is assumed equal to that reported in Ref. [37]. This result confirms that the developed model is sufficiently accurate also as a predictive tool and the neglected phenomena have minor effects; therefore it can be used to provide a further insight into the understanding of the basic principles regulating DMFC operation and as a tool for components optimization.

Modeling results discussion

Water transport through cathode GDL and membrane

Fig. 5(a) illustrates the water fluxes through cathode GDL at different current densities, in the same operating condition of Fig. 8 in Ref. [37]. Liquid permeation does not occur and the only mechanism regulating water transport through cathode GDL is gas diffusion, as expected from the experimental analysis in Section 2. Moreover gas diffusion increases with current density: this implies an increase of water concentration in the electrode, that at low current density is not close to the saturation value. Since liquid permeation does not occur,

DMFC performances are not limited by bulk pores obstruction and cathode flooding manifests itself as a reduction of cathode diffusivity due to superficial pores obstruction [37].

Comparing the water fluxes through the membrane of MEA MM with those of MEA GM (Fig. 8 in Ref. [37]), Fig. 5(b), the main difference concerns the liquid diffusion flux. The presence of anode MPL entails a reduction of liquid water concentration at the membrane interface; as a consequence there is an inversion of liquid diffusion flux, that is directed from the cathode to the anode for current densities higher than 0.4 A cm^{-2}. In the literature the magnitude and direction of diffusion flux is controversial [53,54]: the developed model, validated on the measured water flux at cathode outlet in a wide range of operating conditions, provides a further insight into the understanding of water diffusion through the membrane. Moreover, since model predictions reproduce experimental data with good accuracy, it is confirmed that the neglected mass transfer coefficients for the absorption and desorption of water at membrane-DL interfaces [44,45] have minor effects in the investigated conditions.

Methanol transport through anode DL

In this work methanol transport through anode DL is assumed to be governed by three different transport mechanisms: liquid permeation and gas and liquid diffusion. Fig. 6 illustrates the magnitude of these transport mechanisms along channel length considering a DL without MPL.[1]

At 0.02 A cm^{-2}, Fig. 6(a), all the three mechanisms regulating methanol transport are not negligible. In particular liquid permeation is predominant at the beginning of the channel, while it becomes less important towards channel end, coherently with a reduction of liquid pressure in the channel. Despite the absence of MPL, that reduces liquid saturation, gas diffusion is the main transport mechanisms at channel outlet.

Increasing the current density up to 0.4 A cm^{-2}, Fig. 6(b), the contribution of liquid permeation is not relevant. At the beginning of the channel liquid diffusion sharply decreases coherently with the saturation profile in the channel; however at high current density the main methanol transport mechanisms turns out to be gas diffusion.

The presence of anode MPL affects the magnitude of methanol transport mechanisms. In fact at 0.02 A cm^{-2}, Fig. 7(a), the contribution of gas diffusion is relevant even at low current density and it is not equal to zero at channel inlet, coherently with a reduced value of saturation within the DL. This behavior is more evident at 0.4 A cm^{-2}, where methanol transport is essentially due to gas diffusion. Therefore DL wettability strongly influences mass transport through DL [55,56]: the lower the DL wettability, the lower the magnitude of methanol liquid transport mechanisms.

As proposed in Ref. [52], also in this work methanol crossover is assumed dependent on methanol concentration in the liquid phase and it can be reduced introducing anode MPL, that enhances gas diffusion mechanism. Model predictions, Figs. 6 and 7, are in full agreement with the corresponding methanol crossover measurements reported in Fig. 3. The higher the magnitude of gas diffusion, the lower the methanol liquid concentration in the CL: this implies a reduction of the corresponding methanol crossover flux through the membrane.

Unfortunately a too low methanol concentration in the anode CL can result in a large mass transport loss, worsening cell voltage. Therefore maintaining an adequate methanol concentration in the anode CL is critical to minimize methanol crossover and mass transport loss.

In particular it would be beneficial to reduce methanol liquid concentration within the CL at channel inlet and

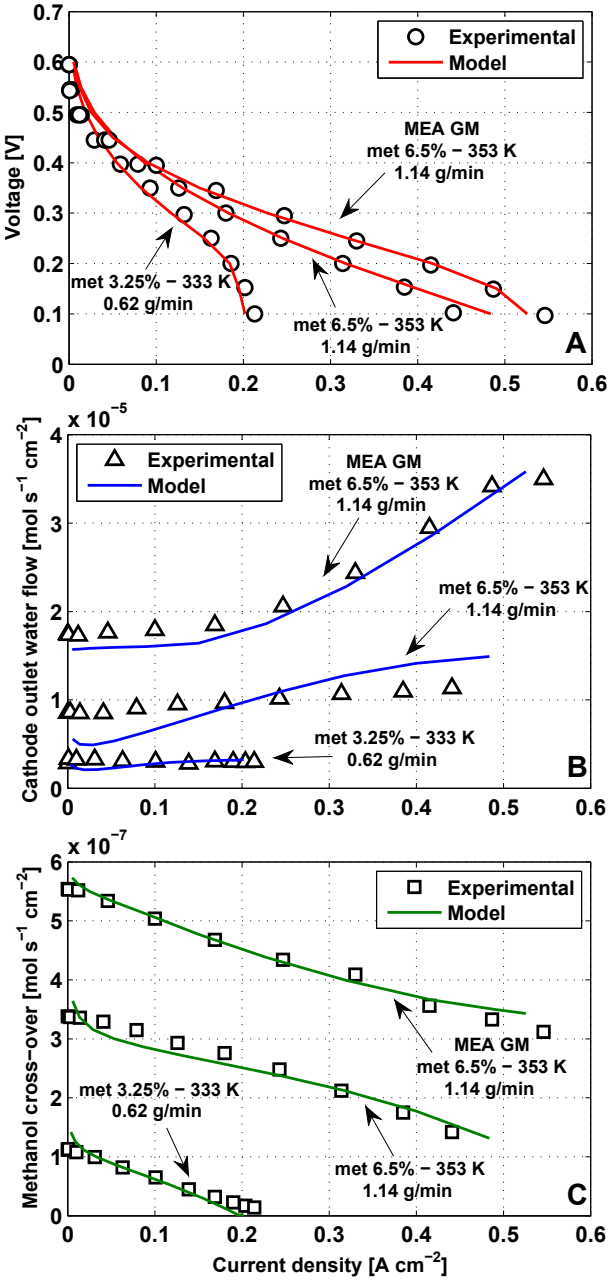

Fig. 4 – Comparison of the simulated and measured a) performance, b) water fluxes at cathode outlet, c) methanol crossover.

[1] The magnitude of methanol transport mechanisms is evaluated at DL interface facing to the CL.

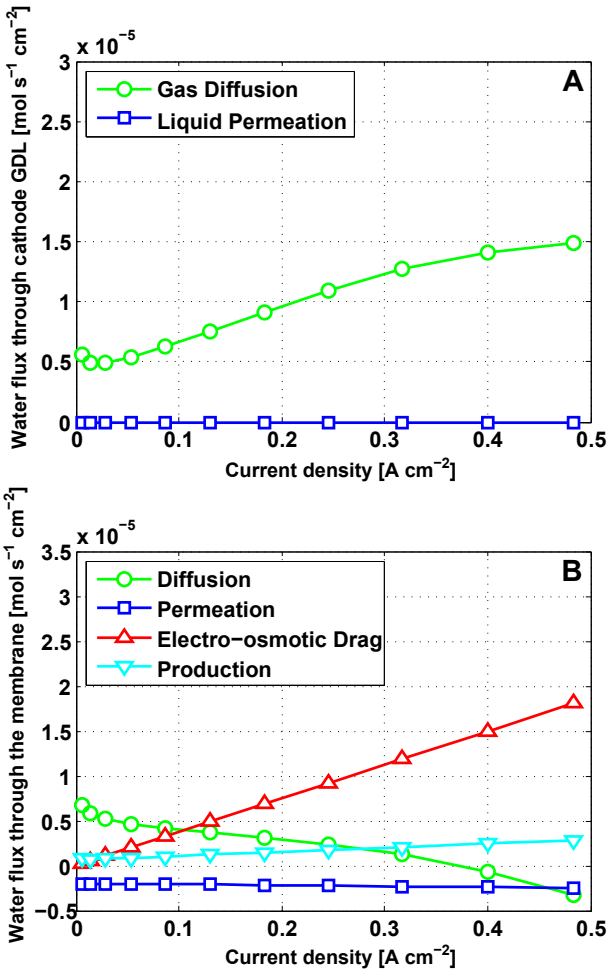

Fig. 5 – Water fluxes through a) cathode GDL, b) membrane (MEA MM, met 6.5%, 353 K, airflow 1.14 g min^{-1}).

increase it towards the channel end. Instead the anode MPL lowers methanol liquid concentration also at channel outlet. This consideration suggests the possibility to design a locally optimized anode DL, characterized by different transport properties along the channel. A suitable solution could be to increase the DL hydrophobicity at channel inlet and reduce it towards channel outlet.

Component optimization

Since the developed model reproduces the experimental data over a wide range of operating conditions with different configurations of anode DL, it can be used as an effective tool to design a locally optimized anode DL.

The manufacturing of a DL with different hydrophobic/hydrophilic properties is a not well consolidated technique, instead it is more practical to realize a DL with a variable thickness of both GDL and MPL. For this reason in the following it is analyzed a DL composed by MPL with a linearly decreasing thickness from 50 μm at channel inlet to 5 μm at channel outlet. Instead the thickness of the GDL is linearly increasing from 200 μm at channel inlet to 245 μm at channel outlet: in this way the total thickness of the anode DL remains constant. This configuration could be obtained for example imposing a variable GDL compression; anyway the technique to practically realize such configuration is out of the scope of this work.

Fig. 8 reports methanol liquid concentration distribution across the DL at a plausible DMFC operating condition, considering three different configuration of anode DL: GDL of constant thickness (250 μm) without MPL, GDL (200 μm) coated with MPL (50 μm) of constant thickness and GDL with MPL of linearly decreasing thickness, as previously described.

In the configuration without the MPL, Fig. 8(a), the value of liquid concentration at the GDL interface facing to the electrode is relatively high: this implies lower anode overpotential (Fig. 9) but also higher methanol crossover (Fig. 10), that increases cathode overpotential. Moreover the concentration at electrode interface presents a considerable gradient from inlet to outlet: this entails a relevant variation of anode overpotential along channel length (Fig. 9), enhancing heterogeneities in DMFC operation. Considering the case of MPL with constant thickness, Fig. 8(b), the behavior is the same of that reported in Fig. 8(a), but the values of concentration are lower due to the additional MPL mass transport resistance. In this configuration the crossover is reduced (Fig. 10), but towards the end of the channel fuel starvation may occur. This is confirmed by a considerable increase of anode overpotential at channel end (Fig. 9).

Utilizing a diffusion layer with MPL of variable thickness, Fig. 8(c), it is possible to obtain a more uniform distribution of

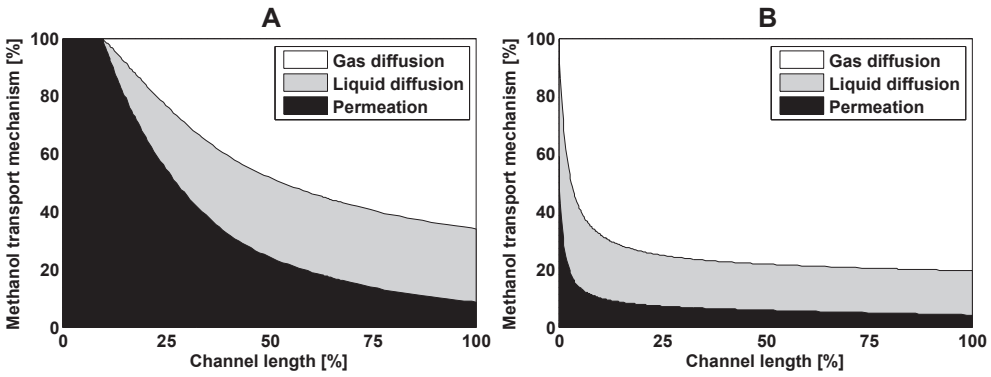

Fig. 6 – Magnitude of methanol transport mechanisms through anode DL along channel length a) $i = 0.02$ A cm^{-2}, b) $i = 0.4$ A cm^{-2} (MEA GM, met 6.5%, 353 K, airflow 1.14 g min^{-1}).

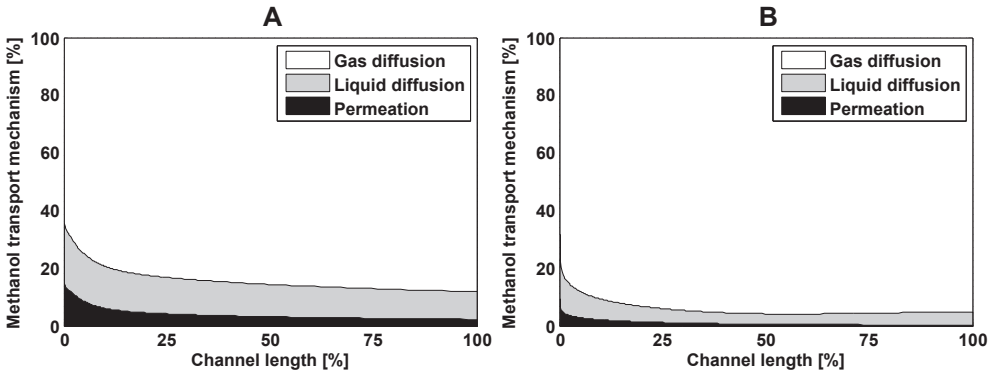

Fig. 7 – Magnitude of methanol transport mechanisms through anode DL along channel length a) $i = 0.02$ A cm^{-2}, b) $i = 0.4$ A cm^{-2} (MEA MM, met 6.5%, 353 K, airflow 1.14 g min^{-1}).

liquid concentration at electrode interface, entailing a more uniform DMFC operation. In fact both the anode overpotential and methanol crossover profiles along channel length become smoother (Figs. 9 and 10) compared with the other options.

The presence of an optimized anode DL could thus improve system lifetime: in fact several degradation mechanisms, such as carbon corrosion and platinum/ruthenium dissolution, directly depend on electrode potential. The reduced gradient of anode potential and methanol crossover, that affects also cathode potential, could limit the severity of local degradation phenomena.

Conclusions

In the present work the effect of anode MPL on DMFC operation is investigated both experimentally and theoretically. The developed 2D two-phase isothermal model includes a detailed description of water and methanol transport through anode DL: the former is regulated by liquid convection, while the latter is governed by both liquid convection and gas and liquid diffusion. The implemented model is able to reproduce accurately the experimental data. Such model is validated by means of three sets of experimental data (polarization curve, methanol crossover, water flow at cathode outlet), in an extensive range of operating conditions with different configurations of anode DL.

The main conclusions on the effects of anode MPL are the followings:

- the presence of the additional MPL mass transport resistance implies that methanol and water crossover are reduced and that water removal from the cathode is mainly governed by gas diffusion; moreover in all the investigated operating conditions no liquid permeation through cathode GDL occurs, as a consequence DMFC performance of MEA MM are not hindered by bulk pores obstruction;
- the presence of anode MPL causes an inversion of liquid diffusion flux through the membrane: at high current densities is directed from the cathode to the anode; however the total water crossover flux is still directed from anode to cathode;

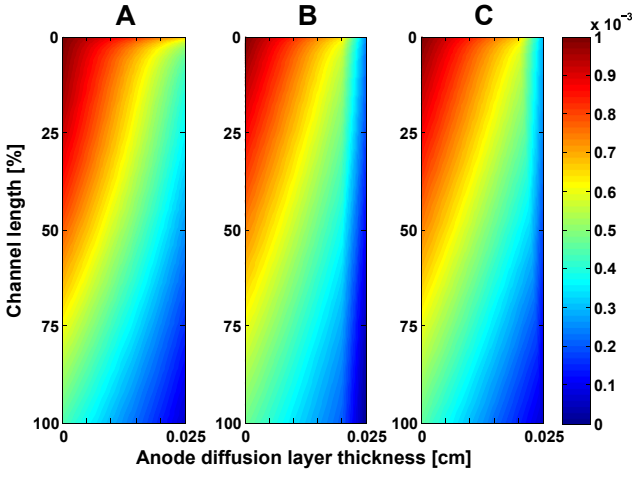

Fig. 8 – Methanol liquid concentration across anode DL at $i = 0.25$ A cm^{-2}, met 3.25%, 353 K, airflow 1.14 g min^{-1}a) GDL of constant thickness, b) GDL + MPL of constant thickness, c) optimized GDL + MPL.

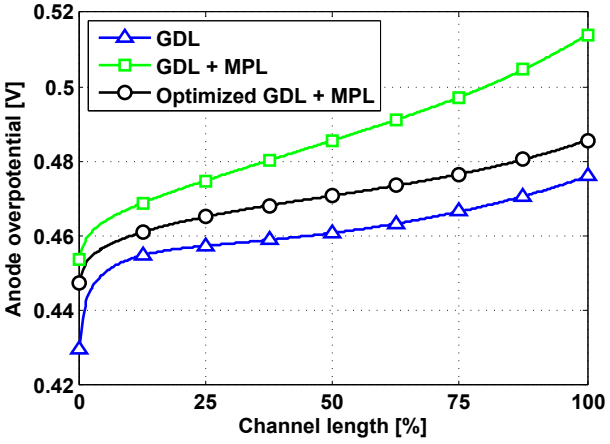

Fig. 9 – Anode overpotential profiles along channel length with different anode DL at $i = 0.25$ A cm^{-2}, met 3.25%, 353 K, airflow 1.14 g min^{-1}.

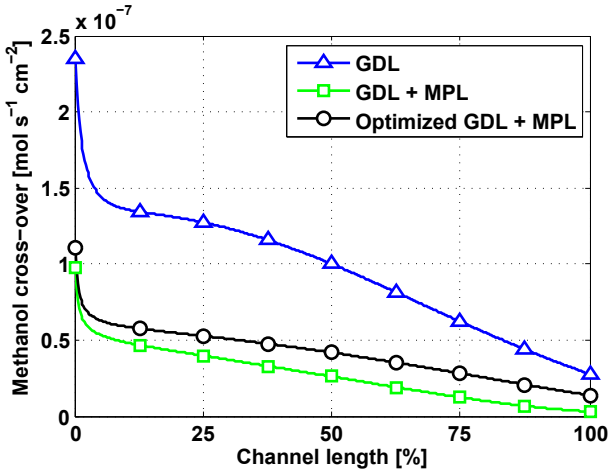

Fig. 10 – Methanol crossover profiles along channel length with different anode DL at $i = 0.25$ A cm^{-2}, met 3.25%, 353 K, airflow 1.14 g min^{-1}.

- without anode MPL, at low current density liquid convection is the predominant methanol transport mechanism at the beginning of the channel, while towards channel end it diminishes and gas diffusion contribution becomes more relevant, instead increasing the current density gas diffusion turns out to be the main methanol transport mechanism along the whole length of the channel;
- with anode MPL, even at low current density the main methanol mass transport mechanisms is gas diffusion, implying a general reduction of methanol crossover;
- model simulations lowering the hydrophobicity of anode DL towards channel end highlight the possibility to design an optimized DL with a reasonable trade-off between low mass transport loss and reduced methanol crossover.

Acknowledgments

This work has been performed in the frame of the FCH-JU FP7 project Premium Act (EC Grant Agreement 256776).

List of symbols

C	species concentration in the channel, mol cm^{-3}
D	diffusivity, cm^2 s^{-1}
R	universal gas constant, J mol^{-1} K^{-1}
T	fuel cell temperature, K
K_H	Henry constant, mol J^{-1}
M	molecular weight, g mol^{-1}
K	permeability, m^2
N_{H_2O}	water flux, mol cm^{-2} s^{-1}
N_{CH_3OH}	methanol flux, mol cm^{-2} s^{-1}
p_c	capillary pressure, Pa
x	x coordinate, cm
s	liquid saturation
J(s)	Leverett function
EW	equivalent weight of ionomer, g mol^{-1}

Greek symbol

σ_{H_2O}	surface tension, N m^{-1}
ρ_{dry}	dry membrane density, g cm^{-3}
μ	compound viscosity, Pa s
ν	compound kinematic viscosity, m^2 s^{-1}
θ_c	contact angle, °
ε	porosity
λ	membrane water content
$\bar{\lambda}$	average membrane water content
σ_m	membrane ionic conductivity, Ω^{-1} cm^{-1}

Superscript

a	relative to anode
c	relative to cathode
t	relative to catalyst layer
G	relative to gas phase
L	relative to liquid phase
DL	relative to diffusion layer

Subscript

DL	relative to diffusion layer
GDL	relative to gas diffusion layer
ch	relative to channel
m	relative to membrane
eq	relative to equilibrium
H_2O	relative to water
CH_3OH	relative to methanol
Int	relative to a layer interface

REFERENCES

[1] Larmine J, Dicks A. Fuel cell systems explained. In: 2nd ed., editor. Chichester, West Sussex: Wiley; 2003.
[2] Aricò AS, Srinivasan S, Antonucci V. DMFCs: from fundamental aspects to technology development. Fuel Cells 2001;1:133–61.
[3] Li X, Faghri A. Review and advances of direct methanol fuel cells (DMFCs) part I: design, fabrication, and testing with high concentration methanol solutions. J Power Sources 2013;226:223–40.
[4] Zhao TS, Xu C, Chen R, Yang WW. Mass transport phenomena in direct methanol fuel cells. Prog Energy Combust Sci 2009;35:275–92.
[5] Jiao K, Li X. Water transport in polymer electrolyte membrane fuel cells. Prog Energy Combust Sci 2011;37:221–91.
[6] Xu C, Zhao TS. In situ measurements of water crossover through the membrane for direct methanol fuel cells. J Power Sources 2007;168:143–53.
[7] Kang S, Lee SJ, Chang H. Mass balance in a direct methanol fuel cell. J Electrochem Soc 2007;154:B1179–85.
[8] Casalegno A, Bresciani F, Groppi G, Marchesi R. Flooding of the diffusion layer in a polymer electrolyte fuel cell: experimental and modelling analysis. J Power Sources 2011;196:10632–9.
[9] Li H, Tang Y, Wang Z, Shi Z, Wu S, Song D, et al. A review of water flooding issues in the proton exchange membrane fuel cell. J Power Sources 2008;178:103–17.
[10] Ahmed M, Dincer I. A review on methanol crossover in direct methanol fuel cells: challenges and achievements. Int J Energy Res 2011;35:1213–28.
[11] Ren X, Springer TE, Zawodzinski TA, Gottesfeld S. Methanol transport through Nafion membranes. Electro-osmotic drag

effects on potential step measurements. J Electrochem Soc 2000;147:466–74.
[12] Chiu YJ. An algebraic semi empirical model for evaluating fuel crossover fluxes of a DMFC under various operating conditions. Int J Hydrogen Energy 2010;35:6418–30.
[13] Sandhu SS, Crowther RO, Fellner JP. Prediction of methanol and water fluxes through a direct methanol fuel cell polymer electrolyte membrane. Electrochim Acta 2005;50:3985–91.
[14] Liu F, Wang CY. Water and methanol crossover in direct methanol fuel cells – effect of anode diffusion media. Electrochim Acta 2008;53:5517–22.
[15] Lu GQ, Wang CY. Electrochemical and flow characterization of a direct methanol fuel cell. J Power Sources 2004;134:33–40.
[16] Peled E, Blum A, Aharon A, Philosoph M, Lavi Y. Novel approach to recycling water and reducing water loss in DMFCs. Electrochem Solid State Lett 2003;6:A268–71.
[17] Oliveira VB, Rangel CM, Pinto AMFR. Water management in direct methanol fuel cells. Int J Hydrogen Energy 2009;34:8245–56.
[18] Wu QX, Zhao TS, Chen R, Yang WW. Effects of anode microporous layers made of carbon powder and nanotubes on water transport in direct methanol fuel cells. J Power Sources 2009;191:304–11.
[19] Luo Z, Chang Z, Zhang Y, Liu Z, Li J. Electro-osmotic drag coefficient and proton conductivity in Nafion membrane for PEMFC. Int J Hydrogen Energy 2010;35:3120–4.
[20] Xu C, He YL, Zhao TS, Chen R, Ye Q. Analysis of mass transport of methanol at the anode of a direct methanol fuel cell. J Electrochem Soc 2006;153:A1358–64.
[21] Lu Z, Daino MM, Rath C, Kandlikar SG. Water management studies in PEM fuel cells, part III: dynamic breakthrough and intermittent drainage characteristics from GDLs with and without MPLs. Int J Hydrogen Energy 2010;35:4222–33.
[22] Kang K, Park S, Gwak G, Jo A, Kim M, Lim YD, et al. Effect of variation of hydrophobicity of anode diffusion media along the through-plane direction in direct methanol fuel cells. Int J Hydrogen Energy 2014;39:1564–70.
[23] Yi JS, Nguyen TV. An along-the-channel model for proton exchange membrane fuel cells. J Electrochem Soc 1998;145:1149–59.
[24] Ge SH, Yi BL. A mathematical model for PEMFC in different flow modes. J Power Sources 2003;124:1–11.
[25] Bahrami H, Faghri A. Review and advances of direct methanol fuel cells: part II: modeling and numerical simulation. J Power Sources 2013;230:303–20.
[26] McIntyre J, Kulikovsky AA, Müller M, Stolten D. Large–scale DMFC stack model: the effect of a condensation front on stack performance. Int J Hydrogen Energy 2013;38:3373–9.
[27] Pauchet J, Prat M, Schott P, Pulloor Kuttanikkad S. Performance loss of proton exchange membrane fuel cell due to hydrophobicity loss in gas diffusion layer: analysis by multiscale approach combining pore network and performance modeling. Int J Hydrogen Energy 2012;37:1628–41.
[28] Xu C, Zhao TS, He YL. Effect of cathode gas diffusion layer on water transport and cell performance in direct methanol fuel cells. J Power Sources 2007;171:268–74.
[29] He YL, Miao Z, Zhao TS, Yang WW. Numerical study of the effect of the GDL structure on water crossover in a direct methanol fuel cell. Int J Hydrogen Energy 2012;37:4422–38.
[30] Xu C, Zhao TS, Yang WW. Modeling of water transport through the membrane electrode assembly for direct methanol fuel cells. J Power Sources 2008;178:291–308.
[31] Pasaogullari U, Wang CY. Liquid water transport in gas diffusion layer of polymer electrolyte fuel cells. J Electrochem Soc 2004;151:A399–406.
[32] Pasaogullari U, Wang CY. Two-phase transport and the role of micro-porous layer in polymer electrolyte fuel cells. Electrochim Acta 2004;49:4359–69.
[33] Xu C, Faghri A. Effect of the capillary property of porous media on the water transport characteristics in a passive liquid-feed DMFC. J Fuel Cell Sci Technol 2010;7.
[34] Li XY, Yang WW, He YL, Zhao TS, Qu ZG. Effect of anode micro-porous layer on species crossover through the membrane of the liquid-feed direct methanol fuel cells. Appl Therm Eng 2012;48:392–401.
[35] Shaffer CE, Wang CY. Role of hydrophobic anode MPL in controlling water crossover in DMFC. Electrochim Acta 2009;54:5761–9.
[36] Casalegno A, Marchesi R, Parenti D. Two-phase 1D + 1D model of a DMFC: development and validation on extensive operating conditions range. Fuel Cells 2008;8:37–44.
[37] Zago M, Casalegno A, Santoro C, Marchesi R. Water transport and flooding in DMFC: experimental and modeling analyses. J Power Sources 2012;217:381–91.
[38] Casalegno A, Santoro C, Rinaldi F, Marchesi R. Low methanol crossover and high efficiency direct methanol fuel cell: the influence of diffusion layers. J Power Sources 2011;196:2669–75.
[39] Weber AZ, Darling RM, Newman J. Modeling two-phase behavior in PEFCs. J Electrochem Soc 2004;151:A1715–27.
[40] Wang X, Nguyen TV. Modeling the effects of the microporous layer on the net water transport rate across the membrane in a PEM fuel cell. J Electrochem Soc 2010;157:B496–505.
[41] Yang WW, Zhao TS, Chen R, Xu C. An approach for determining the liquid water distribution in a liquid-feed direct methanol fuel cell. J Power Sources 2009;190:216–22.
[42] Weber AZ, Newman J. Transport in polymer-electrolyte membranes – I. Physical model. J Electrochem Soc 2003;150:A1008–15.
[43] Weber AZ, Newman J. Transport in polymer-electrolyte membranes – II. Mathematical model. J Electrochem Soc 2004;151:A311–25.
[44] Ge S, Li X, Yi B, Hsing IM. Absorption, desorption, and transport of water in polymer electrolyte membranes for fuel cells. J Electrochem Soc 2005;152:A1149–57.
[45] Majsztrik PW, Satterfield MB, Bocarsly AB, Benziger JB. Water sorption, desorption and transport in Nafion membranes. J Membr Sci 2007;301:93–106.
[46] Springer TE, Zawodzinski TA, Gottesfeld S. Polymer electrolyte fuel cell model. J Electrochem Soc 1991;138:2334–42.
[47] Meier F, Eigenberger G. Transport parameters for the modelling of water transport in ionomer membranes for PEM-fuel cells. Electrochim Acta 2004;49:1731–42.
[48] Wang ZH, Wang CY. Mathematical modeling of liquid-feed direct methanol fuel cells. J Electrochem Soc 2003;150:A508–19.
[49] Zago M, Casalegno A. A physical model of direct methanol fuel cell anode impedance. J Power Sources 2014;248:1181–90.
[50] Tschinder T, Schaffer T, Fraser SD, Hacker V. Electro-osmotic drag of methanol in proton exchange membranes. J Appl Electrochem 2007;37:711–6.
[51] Zawodzinski TA, Derouin C, Radzinski S, Sherman RJ, Smith VT, Springer TE, et al. Water uptake by and transport through Nafion 117 membranes. J Electrochem Soc 1993;140:1041–7.
[52] Casalegno A, Marchesi R. DMFC performance and methanol cross-over: experimental analysis and model validation. J Power Sources 2008;185:318–30.

[53] Ren X, Springer TE, Gottesfeld S. Water and methanol uptakes in nafion membranes and membrane effects on direct methanol cell performance. J Electrochem Soc 2000;147:92–8.
[54] Oedegaard A, Hentschel C. Characterisation of a portable DMFC stack and a methanol-feeding concept. J Power Sources 2006;158:177–87.
[55] Gauthier E, Duan Q, .Hellstern T, Benziger J. Water flowing, through, and around the gas diffusion layer. Fuel Cells 2012;12:835–47.
[56] Sinha PK, Mukherjee PP, Wang CY. Impact of GDL structure and wettability on water management in polymer electrolyte fuel cells. J Mater Chem 2007;17:3053–272.